

# Electrochemical Oxidation of the Phospha- and Arsaethynolate Anions, $\text{PCO}^-$ and $\text{AsCO}^-$

Frank Tambornino<sup>+, [a]</sup> Eden E. L. Tanner<sup>+, [b, c]</sup> Hatem M. A. Amin<sup>+, [b]</sup> Jennifer Holter<sup>, [d]</sup> Tim Claridge<sup>, [a]</sup> Richard G. Compton<sup>, [b], \*</sup> and Jose M. Goicoechea<sup>, [a], \*</sup>

**Abstract:** The anions  $\text{PCO}^-$  and  $\text{AsCO}^-$  are shown to be electroactive and are studied in aqueous and non-aqueous solutions. Cyclic voltammetry is used to extract fundamental physico-chemical parameters such as oxidation peak potentials, and transfer and diffusion coefficients of the anions to better understand the nature of the oxidation process. Variation of the potential scan rate reveals that electro-oxidation of  $\text{PCO}^-$  with the release of CO is controlled by diffusion and is a one-electron irreversible process yielding phosphorus-containing deposits. In contrast, the oxidation of  $\text{AsCO}^-$  is a near electrochemically reversible process, forming pure arsenic deposits, with a chemically irreversible follow-up reaction. For both anions, the electrode surface is substantially “blocked” by the reaction products. The formed deposits were characterized by scanning electron microscopy and energy dispersive X-ray spectroscopy.

**Introduction:** Phosphorus compounds, and to a lesser extent their arsenic analogues, are of relevance in a wide range of industrial and biological applications.<sup>[1]</sup> During the last decade, the phosphorus- and arsenic-containing analogues of cyanate, specifically the 2-phosphaethynolate ( $\text{PCO}^-$ ) and 2-arsaethynolate ( $\text{AsCO}^-$ ) ions, have gradually become important chemical precursors to novel compounds.<sup>[2,3]</sup>  $\text{PCO}^-$ , first reported by Becker *et al.* in 1992,<sup>[3a]</sup> is remarkably stable when isolated as a sodium or potassium salt allowing for its study in aqueous solution. In recent years, the phosphaethynolate ion has been most commonly used as  $[\text{Na}(\text{dioxane})]\text{PCO}$  as it can be conveniently prepared on a multi-gram scale from the phosphide ion ( $\text{PH}_2^-$ ) and a carbonate source.<sup>[4]</sup> In 2016, its heavier analogue, the  $\text{AsCO}^-$  anion, was isolated as  $[\text{Na}(18\text{-crown-6})]\text{AsCO}$  by Hinz and Goicoechea,<sup>[5a]</sup> and akin to its lighter homologue, the synthesis of  $[\text{Na}(\text{dioxane})]\text{AsCO}$  is facile

and feasible on large scale.<sup>[5]</sup> Over the last years, these species have been employed as versatile precursors to novel and rare phosphorous- and arsenic-containing compounds.<sup>[2–7]</sup> By decarbonylation,  $\text{PCO}^-$  and  $\text{AsCO}^-$  anions may act as a source of monoanionic pnictogen ions (“P<sup>–</sup>” or “As<sup>–</sup>”, respectively).<sup>[2]</sup> These reactions proceed under thermal or photolytic conditions either in a dissociation or intramolecular rearrangement reaction, as the release of CO gas is thermodynamically favoured.<sup>[2–7]</sup> Although these results support the possibility of using  $\text{PCO}^-$  and  $\text{AsCO}^-$  as precursors for meta-stable clusters, careful optimization of the reaction conditions is needed to limit the decomposition of such compounds to the corresponding elemental pnictogen.<sup>[2]</sup>

It has been shown experimentally, that both  $\text{PCO}^-$  and  $\text{AsCO}^-$  are readily oxidized. Reaction of  $\text{PCO}^-$  with  $\text{SO}_2$  leads to formation of the  $\text{P}_4\text{C}_4\text{O}_4^{2-}$  tetramer which exhibits a bicyclic butterfly like structure with a central P–P bond.<sup>[3b]</sup>  $\text{AsCO}^-$  oxidizes in air to give elemental arsenic. Side products of reactions involving  $\text{AsCO}^-$  have been shown to contain  $\text{As}_{10}^{2-}$  and  $\text{As}_{12}^{4-}$ , products stemming from partial oxidation of  $\text{AsCO}^-$ .<sup>[5a]</sup> A single electron oxidation of these anions would theoretically yield the neutral radicals  $\text{PCO}^\bullet$  and  $\text{AsCO}^\bullet$ , respectively. Although  $\text{PCO}^\bullet$  has been isolated in an argon matrix and studied by negative ion photoelectron spectroscopy, it is unstable as bulk substance.<sup>[8]</sup> Reduction of  $\text{PCO}^-$  with  $\text{KC}_8$  in the coordination sphere of  $\text{Sc}^{3+}$  leads to a dinuclear complex bridged by the  $(\text{OCPPCO})^{4-}$  ligand.<sup>[9]</sup> By contrast, reduction with a uranium(III) compound affords a bimetallic oxo-bridged species with a terminal  $\text{CP}^-$  ligand on one of the uranium centers.<sup>[10]</sup>

Electrochemistry offers a useful and effective tool to understand redox chemistry and the associated thermodynamic and mechanistic information,<sup>[11]</sup> however the measurement of electrochemical properties of the  $\text{PCO}^-$  anion has received scarce attention;<sup>[3c]</sup> whereas the electrochemical behaviour of the  $\text{AsCO}^-$  anion has not been reported. This prompted us to investigate the fundamental electrochemistry of  $\text{PCO}^-$  and  $\text{AsCO}^-$ . We show that both are electroactive and form deposits upon electro-oxidation, respectively. The electrochemical oxidation of  $\text{PCO}^-$  and  $\text{AsCO}^-$  is investigated in aqueous and non-aqueous electrolytes using cyclic voltammetry. Significant information on the nature of the oxidation process and important physico-chemical parameters such as transfer coefficients and diffusion coefficients of the anions were extracted from studying the variation of the potential scan rate. The morphology and the composition of the electrode surface were examined using scanning electron microscopy (SEM) and energy dispersive X-ray spectroscopy (EDX) in order to probe the nature of the deposits formed. Whereas an ill-defined phosphorus-containing product was observed on oxidation of  $\text{PCO}^-$ , oxidation of  $\text{AsCO}^-$  affords a compositionally pure coating of arsenic.

[a] Dr. F. Tambornino, Prof. Dr. T. Claridge, Prof. Dr. J. M. Goicoechea  
Department of Chemistry, University of Oxford  
Chemistry Research Laboratory  
12 Mansfield Road, Oxford, OX1 3TA, United Kingdom  
E-mail: jose.goicoechea@chem.ox.ac.uk

[b] Dr. E. E. L. Tanner, Dr. H. M. A. Amin, Prof. Dr. R. G. Compton  
Department of Chemistry, University of Oxford  
Physical and Theoretical Chemistry Laboratory  
South Parks Road, Oxford, OX1 3QZ, United Kingdom  
E-mail richard.compton@chem.ox.ac.uk

[c] Dr. E. E. L. Tanner  
New address: School of Engineering & Applied Sciences, Harvard  
University, Cambridge, MA, USA.

[d] Mrs. J. Holter  
Department of Materials, University of Oxford  
Parks Road, Oxford, OX1 3PH, United Kingdom

\* These authors contributed equally to this work

Supporting information for this article is given via a link at the end of the document.

**Electrochemical oxidation of  $\text{PCO}^-$  in aqueous and non-aqueous solutions:** The aqueous electrochemistry of  $\text{PCO}^-$  in a solution of 0.1 M KCl was investigated by submerging a glassy carbon (GC) working electrode, Pt-sponge counter electrode and Ag pseudo-reference electrode into a deoxygenated solution of 2.0 mM NaPCO in 0.1 M KCl. Subsequently, a cyclic voltammogram was recorded by sweeping the potential from 0.0 V to 1.1 V and back to 0.0 V (vs. Ag reference). A peak appeared on the forward scan at ca. 0.85 V vs. Ag, whilst no peak was seen on the reverse scan even at low potentials. This behaviour is related to the formation of insoluble products on the GC electrode surface which can be compared with a reported irreversible oxidation of NaPCO in DMSO containing  $\text{tBu}_4\text{NBF}_4$  as electrolyte, which was interpreted, in part, to the possible formation of insoluble  $(\text{P}_4\text{C}_4\text{O}_4)^{2-}$  anion.<sup>[3b]</sup> Next we recorded cyclic voltammetry (CV) over a range of scan rates (from 10–1000  $\text{mV s}^{-1}$ ) as shown in Figure 1.

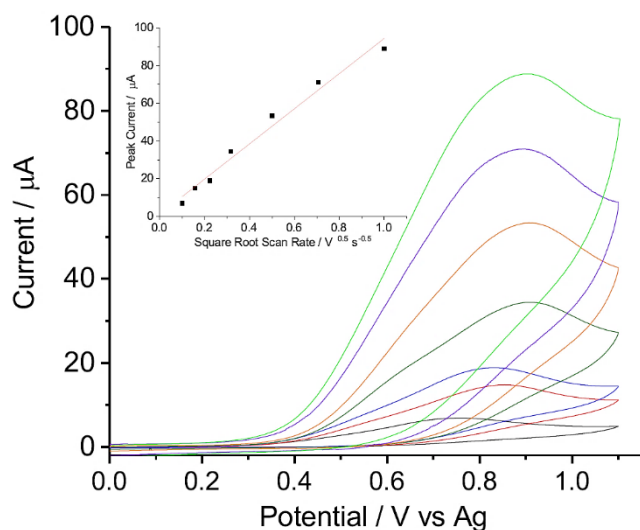


**Figure 1.** CV of 2.0 mM NaPCO in 0.1 M KCl recorded at 10  $\text{mV s}^{-1}$  (black), 25  $\text{mV s}^{-1}$  (red), 50  $\text{mV s}^{-1}$  (blue), 100  $\text{mV s}^{-1}$  (olive), 250  $\text{mV s}^{-1}$  (orange), 500  $\text{mV s}^{-1}$  (violet), and 1000  $\text{mV s}^{-1}$  (green). Inset is a plot of the peak current vs. square root of the scan rate.  $R^2 = 0.980$ .

As can be seen from the inset of Figure 1, the peak current increased linearly with the square root of the scan rate, indicating a diffusion controlled process. Tafel slopes can be constructed by taking the natural logarithm of the current and measuring the slope of the portion of the curve that is controlled by electron transfer kinetics (avoiding the diffusion controlled part of the process). From this, the transfer coefficient,  $\beta$ ,<sup>[12]</sup> which describes phenomenologically whether the transition state is more product-like or reactant like, can be calculated:

$$\beta = \frac{\text{Tafel slope} \times RT}{F} \quad (1)$$

where  $R$  is the Universal Gas Constant ( $8.314 \text{ J K}^{-1} \text{ mol}^{-1}$ ),  $T$  is the temperature in K (298 K), and  $F$  is Faraday's constant

( $96485 \text{ C mol}^{-1}$ ). This gives  $\beta$  of  $0.24 \pm 0.01$  as averaged across all of the scan rates, suggesting that the process is consistent with a one electron electrochemically irreversible process, with the transition state being closer to the starting anion in character. The irreversible Randles-Sevcik equation (Equation 2) can then be employed to calculate the diffusion coefficient of  $\text{PCO}^-$ :

$$\frac{i_p}{\nu^{0.5}} = 2.99 \times 10^5 A D^{0.5} C n (n' + \beta)^{0.5} \quad (2)$$

where  $A$  is the area of the electrode,  $C$  is the bulk concentration (here 2.0 mM),  $n'$  is the number of electrons transferred before the rate determining step (here assumed to be 0),  $n$  is the overall number of electrons (here 1),  $i_p \nu^{0.5}$  is the slope of the plot shown in the inset of Figure 1, and  $\beta$  is the transfer coefficient (as introduced above). This gives a diffusion coefficient for  $\text{PCO}^-$  in water of  $(1.8 \pm 0.3) \times 10^{-9} \text{ m}^2 \text{ s}^{-1}$ . Diffusion NMR Spectroscopy was used to independently determine the diffusion coefficient by tracking the  $^{31}\text{P}$  signal. This measurement gave a diffusion coefficient of  $(1.7 \pm 0.01) \times 10^{-9} \text{ m}^2 \text{ s}^{-1}$ , in excellent agreement with the electrochemical measurement.

The aqueous electrochemical behaviour of  $\text{PCO}^-$  was also explored using Pt and Au working electrodes; however passivation of the electrode surfaces gave rise to a weak electrochemical response relative to the GC electrode (see Figure S1). This effect is most likely due to the different adsorption strengths of  $\text{PCO}^-$  and the oxidation intermediates/products on the electrode surfaces.

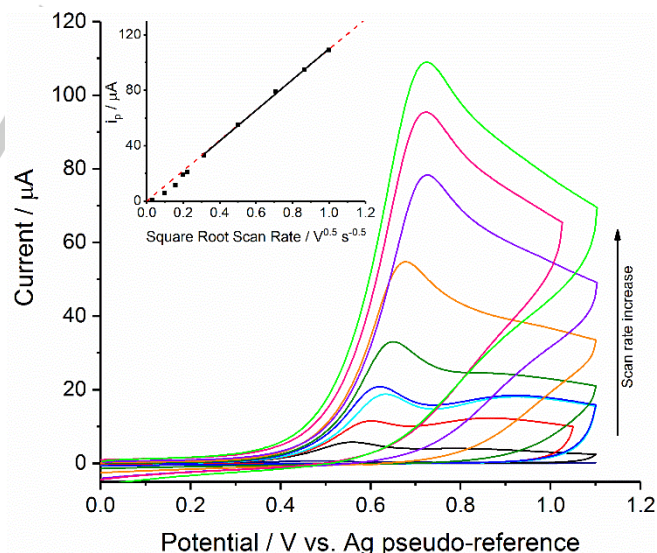


**Figure 2.** CV of 2.0 mM NaPCO in 0.1 M [Pmim][NTf<sub>2</sub>] in MeCN recorded at 1  $\text{mV s}^{-1}$  (navy), 10  $\text{mV s}^{-1}$  (black), 25  $\text{mV s}^{-1}$  (red), 40  $\text{mV s}^{-1}$  (cyan), 50  $\text{mV s}^{-1}$  (blue), 100  $\text{mV s}^{-1}$  (olive), 250  $\text{mV s}^{-1}$  (orange), 500  $\text{mV s}^{-1}$  (violet), 750  $\text{mV s}^{-1}$  (pink) and 1000  $\text{mV s}^{-1}$  (green). Inset is a plot of the peak current vs. square root of the scan rate.  $R^2 = 0.998$

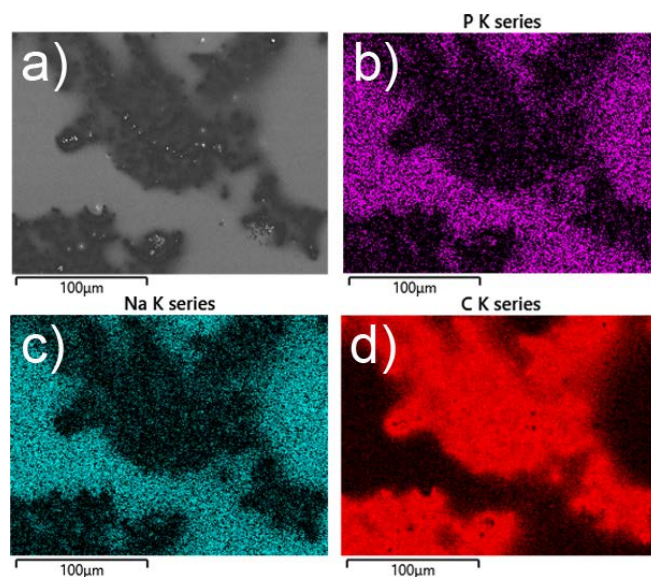


Next, the above electrochemical process was repeated with NaPCO dissolved in acetonitrile with 0.1 M [Pmim][NTf<sub>2</sub>] as the supporting electrolyte ([Pmim][NTf<sub>2</sub>] = 1-propyl-3-methylimidazolium bis(trifluoromethylsulfonyl)imide). The ionic liquid was selected as supporting electrolyte to minimise ion pairing with the PCO<sup>-</sup> anion. The electrodes were immersed in the solution and a CV was recorded by scanning the potential from 0.0 V to 1.1 V and back to 0.0 V across a range of scan rates (1–1000 mV s<sup>-1</sup>) as shown in Figure 2. An oxidation peak appears at ca. 0.7 V (vs. Ag pseudo-reference) on the forward scan, whilst no peaks were observed on the reverse scan. The oxidation potential of PCO<sup>-</sup> in non-aqueous solution is ca. 200 mV less positive than that in aqueous electrolyte. A plot of peak current vs square root of the scan rate was constructed (inset of Figure 2) showing a linear behaviour for scan rates greater than 100 mV s<sup>-1</sup>, suggesting, again, that the process is controlled by diffusion. At lower scan rates, the electrode is passivated by the product of the oxidation, resulting in a measured peak current lower than expected. Note that the effects of electrode blocking are scan rate dependent reflects the relative size of the diffusion layer and the size of the insulating blocking material.<sup>[13]</sup>

Values for the transfer coefficient were determined by measurement of the Tafel slope and application of Equation 1 to give  $\beta = 0.30 \pm 0.02$  (Figure S2). The irreversible Randles-Sevcik equation (Equation 2) was once again used and gave a diffusion coefficient for PCO<sup>-</sup> in MeCN of  $(2.3 \pm 0.3) \times 10^{-9} \text{ m}^2 \text{ s}^{-1}$ . Again, Diffusion NMR Spectroscopy was used to independently determine the diffusion coefficient by tracking the <sup>31</sup>P signal giving a diffusion coefficient of  $(2.3 \pm 0.01) \times 10^{-9} \text{ m}^2 \text{ s}^{-1}$ .

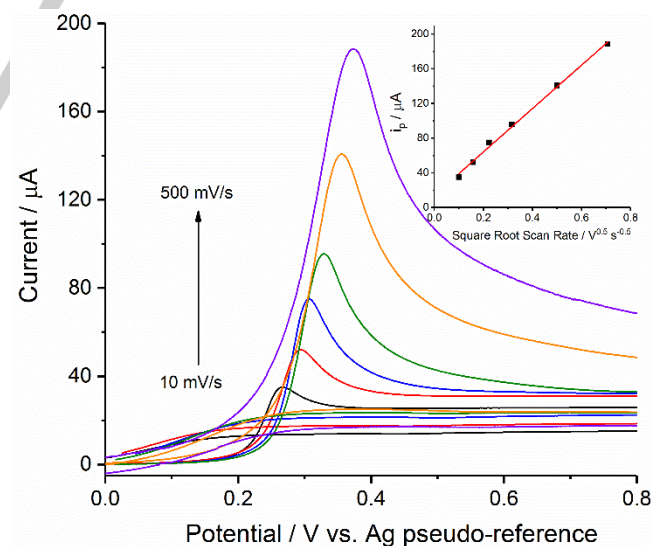
The above results imply that PCO<sup>-</sup> is electrochemically oxidized in an irreversible process yielding phosphorus-containing deposits. These insoluble deposits block the electrode surface and inhibit further electrochemical response on subsequent scans (consequently the working electrode must be polished between measurements). In order to investigate the deposition of phosphorus-containing material during the electro-oxidation of NaPCO, SEM and EDX were used. SEM images were recorded on a Zeiss Merlin Field Emission Gun (FEG)-SEM, at an acceleration voltage of 5 kV. Images were recorded after conducting 50 potential scans between 0 V and 1 V (vs. Ag pseudo reference electrode) and washing the electrode with MeCN.

Figure 3a shows an SEM image of the electrode deposits which consists a layer of micro particles (bright area and spots in the image). The EDX spectra of the deposits exclusively show peaks corresponding to P, Na, O and C. Given that the working electrode is GC, we are unable to quantify the amount of C in the sample. The EDX analysis rules out the formation of a pure phosphorus layer, see Figure S3, and suggests that Na:P:O are present in the sample in approximately a 2:3:5 ratio. The insolubility of this deposit precludes any further analysis. EDX elemental mapping (Figure 3b, c and d) also shows the overlay of the maps for Na and P elements, indicating the presence of residual salt particles on the electrode.



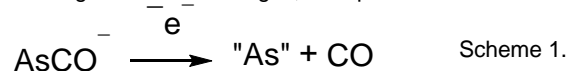
**Figure 3.** (a) SEM image of the GC electrode after electrochemical potential sweeping between 0 V and 1 V for 50 scans in 2.0 mM PCO<sup>-</sup> solution and then washing. EDX elemental map showing the distribution of (b) P, (c) Na and (d) C. For the corresponding EDX spectrum see SI.

**Electrochemical oxidation of AsCO<sup>-</sup> in non-aqueous electrolyte:** NaAsCO is not stable in aqueous electrolytes,<sup>[5]</sup> and thus is only studied in non-aqueous electrolyte. A solution of 2.0 mM NaAsCO in acetonitrile with 0.1 M [Pmim][NTf<sub>2</sub>] was prepared. Electrodes were immersed into the solution prior to a CV being recorded from 0.0 V to 0.8 V at scan rates of 10–500 mV s<sup>-1</sup> (Figure 4).



**Figure 4.** CV of 2.0 mM NaAsCO in 0.1 M [Pmim][NTf<sub>2</sub>] in MeCN recorded at 10 mV s<sup>-1</sup> (black), 25 mV s<sup>-1</sup> (red), 50 mV s<sup>-1</sup> (blue), 100 mV s<sup>-1</sup> (olive), 250 mV s<sup>-1</sup> (orange), and 500 mV s<sup>-1</sup> (violet). Inset is a plot of the peak current vs. square root of the scan rate.  $R^2 = 0.996$ .

A peak appears on the forward scan at ca. 0.2–0.4 V vs. Ag pseudo-reference, whilst no peaks appear on the reductive scan. This peak corresponds to the electro-oxidation of  $\text{AsCO}^-$ , forming arsenic and CO gas, as represented in Scheme 1.



A plot of the peak current vs. the square root of the scan rate is shown in the inset of Figure 4, which shows a linear response ( $R^2 = 0.996$ ) across all recorded scan rates, suggesting that the process is controlled by diffusion of the  $\text{AsCO}^-$  anion to the electrode. Tafel slopes were constructed, and Equations 1 and 2 were once again employed to give a transfer coefficient and a diffusion coefficient of  $0.93 \pm 0.03$  and  $(3.8 \pm 0.3) \times 10^{-9} \text{ m}^2 \text{ s}^{-1}$ , respectively (Figure S4). The value of  $\beta$  (approaching unity) suggests that this is a near electrochemically reversible process, and that the absent back peak indicates follow up chemistry of the electrochemically generated product. This therefore allows the potential measured here to be considered approximately as *thermodynamic* potentials. The variation of the peak potential with scan rate likely reflects that the follow up kinetics shifts the observed peak potential to less positive potential values as the scan rate decreases, which is consistent with an electrochemically reversible process followed by an irreversible chemical follow-up reaction.<sup>[14]</sup>

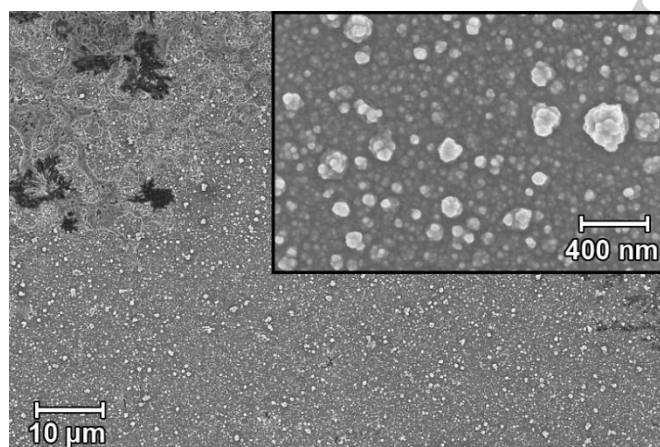


**Figure 5.** SEM image of arsenic-deposits obtained after electrochemical cycling the electrode between 0 V and 1 V for 50 scans in 2.0 mM  $\text{AsCO}^-$  solution. Insert shows a zoom-in SEM image. For the corresponding EDX spectrum see Figure S4.

In order to confirm the deposition of pure arsenic during the electro-oxidation of  $\text{AsCO}^-$ , the surface of the electrode was examined after 50 potential scans by SEM and EDX techniques. Figure 5 shows a representative SEM image of the deposits on the substrate. A compact deposit, which composes of spheroidal and irregular-shaped particles, is formed and the particle size is in the range of 25–100 nm, as can be observed in an enlarged image, see inset of Figure 5. Some of the particles tend to aggregate. The corresponding EDX spectrum of the lower part of Figure 5 shows the appearance of a main peak corresponding

to arsenic, confirming that the obtained deposits are pure arsenic (Figure S5). These results support our discussion of the oxidation of  $\text{AsCO}^-$ , depositing elemental arsenic and evolving CO gas. As a result, the electrode is substantially “blocked” after very few cycles. It is noteworthy to mention that by dipping the electrode in the same  $\text{AsCO}^-$  solution without any electrochemical potential cycling, only residuals of the electrolyte sticking to the electrode were found and no elemental arsenic was observed.

Washing the deposits before imaging is an important step to remove the residual electrolyte solution away from the arsenic deposits and/or substrate. However, at the boundary between the immersed part of the electrode and the undipped part, still a porous layer like a net of the remaining electrolyte is observed onto the underlying arsenic-deposits (Figure S5a), and therefore a signal for Na from the salt appears in the EDX data of region 2, see Figure S5b.

From the above results, electrochemistry demonstrates the oxidation of  $\text{PCO}^-$  and  $\text{AsCO}^-$  anions to phosphorus and arsenic-containing deposits, respectively, with the release of CO; the potentials indicate the ease of the process being under kinetic control in the case of  $\text{PCO}^-$  and near- thermodynamic control for  $\text{AsCO}^-$ .

**Conclusions:** We demonstrated the electrochemical oxidation of  $\text{PCO}^-$  and  $\text{AsCO}^-$  anions in aqueous and non-aqueous electrolytes. Cyclic voltammetry showed the oxidation of these anions at relatively low potentials with loss of carbon monoxide and formation of phosphorus-containing deposits and pure arsenic deposits as the reaction products. SEM and EDX analysis of the electrode surface confirmed the formation of such deposits. The formed deposits thus partially “block” the electrode surface. Variation of the potential scan rate revealed that the oxidation process is diffusion-controlled. Transfer coefficients of the oxidation of  $\text{PCO}^-$  and  $\text{AsCO}^-$  in non-aqueous electrolyte are ca. 0.3 and 0.9, respectively, suggesting that the oxidation of  $\text{PCO}^-$  is a one-electron irreversible process, whilst that of  $\text{AsCO}^-$  is a near electrochemically reversible process followed by an irreversible chemical follow-up reaction.

## Experimental Section

**Chemical Reagents and Synthesis:** Ferrocene ( $\text{Fe}(\text{C}_5\text{H}_5)_2$ , Sigma Aldrich, 98%) and potassium chloride (KCl, Sigma Aldrich, 99%) were used as received. Acetonitrile (MeCN, Fischer Scientific, HPLC grade, 99%) was purified using an MBraun SPS-800 solvent system. Ionic liquid 1-propyl-3-methylimidazolium bis(trifluoromethylsulfonyle)imide ([Pmim][NTf<sub>2</sub>]) was kindly donated by Professor C. Hardacre, School of Chemical Engineering & Analytical Science, Manchester University and was used as received. Argon (99.9%) was purchased from BOC, Surrey, UK. Aqueous solutions were made up in nanopure water with a resistivity not less than 18.2 MΩ cm at 25 °C Millipore, UK). All chemical synthesis reactions were carried out under inert argon or nitrogen atmosphere using standard Schlenk-line or glove box techniques.  $\text{PCO}^-$  anion, synthesized in the form of  $[\text{Na}(\text{dioxane})_x]\text{PCO}$  ( $x = 2$ ), was prepared following the procedure from Heift *et al.*<sup>[4]</sup>  $[\text{Na}(\text{dioxane})_x]\text{AsCO}$  ( $x = 5.6$ ) was synthesized and isolated following the procedure reported by Hinz and Goicoechea.<sup>[5a]</sup> A similar synthetic procedure was applied for both



anions. Briefly, a reaction mixture of sodium and red phosphorus or arsenic (in a molar ratio of 3:1) in dimethoxyethane (DME) with catalytic amounts of naphthalene led to the formation of a black suspensions of Na<sub>3</sub>P or Na<sub>3</sub>As, respectively. Subsequently, a protonation step using *tert*-butanol, followed by carbonylation using diethylcarbonate affords PCO<sup>−</sup> and AsCO<sup>−</sup> solutions, respectively. The solutions were then dried in vacuum, the residues redissolved in THF and the anions in question precipitated with dioxane as their respective [Na(dioxane)<sub>x</sub>]<sup>+</sup> salts. The dioxane content was determined by <sup>31</sup>P-NMR (PCO<sup>−</sup>, PPh<sub>3</sub> as external standard) or <sup>1</sup>H-NMR (AsCO<sup>−</sup>, naphthalene as external standard). The structure of the anions was confirmed by <sup>31</sup>P and <sup>13</sup>C-NMR spectroscopy. For characterization data see ref. 4 and 5.

**Instrumentation:** Electrochemical experiments (Cyclic Voltammetry (CV)) were conducted using a μ-Autolab potentiostat (Eco-Chemie, Netherlands). All experiments were conducted inside a temperature controlled Faraday cage.<sup>[15]</sup> The working glassy carbon (GC) macroelectrode (1.5 × 10<sup>−3</sup> m radius, BASi Analytical, USA) was polished prior to each CV scan on white lapping pads (Buehler, USA) with diamond spray (3.0, 1.0, 0.1 μm from Kemet, Kent, UK, three minutes on each size in a descending order). A platinum mesh was used as a counter electrode, whilst an Ag wire was used as a pseudo-reference electrode. The potentials can be converted onto a scale vs. Fc/Fc<sup>+</sup> considering that the formal potential of Fc/Fc<sup>+</sup> redox couple is 1.36 V vs. Ag-pseudo reference electrode, as determined experimentally in 0.1 M [Pmim][NTf<sub>2</sub>]/MeCN.

For the experiments recorded in acetonitrile solvent, the environment was nominally oxygen free (prepared in a glove box, degassed with argon and transferred to a flushed flask by cannula), and the solution was replaced fresh for each experiment.

Samples for NMR were prepared as solutions of 2.0 mM NaPCO in D<sub>2</sub>O and d<sub>3</sub>-acetonitrile, respectively. <sup>31</sup>P diffusion coefficients were measured at 298 K on a Bruker AVIIIHD 500 NMR spectrometer equipped with a triple resonance BB<sup>1</sup>H/<sup>19</sup>F probe. Measurements were made with the bipolar variant of the stimulated echo including a longitudinal Eddy current delay (LED) period (Bruker ledbpgp2s sequence). Diffusion times Δ were 100 ms and diffusion encoding gradients δ 4 ms with recycle delays of 5s. 16 gradient points were collected using smoothed-square gradient profiles (SMSQ) with strengths ranging from 1–25 G/cm, each of 16 transients. Data were fitted to the Stejskal-Tanner equation using the Bruker T1T2 fitting routines in TOPSPIN 3.5.<sup>[16]</sup>

## Acknowledgements

H. M. A. Amin and F. Tambornino gratefully acknowledge the DFG for funding (No. AB 702/1-1 and No. FT 1357/1-1). The research leading to these results has received partial funding from the European Research Council under the European Union's Seventh Framework Programme (FP/2007-2013)/ERC Grant Agreement no. [320403].

**Keywords:** Phosphaethynolate • Arsaethnolate • Phosphorus • Arsenic • Electrochemical Oxidation

- [1] a) H. Diskowski, T. Hofmann, *Ullmann's Encyclopedia of Industrial Chemistry* **2000**; b) S. C. Grund, K. Hanusch, H. U. Wolf, *Ullmann's Encyclopedia of Industrial Chemistry* **2008**; c) E.-C. Koch, *Propellants, Explosives, Pyrotechnics* **2008**, 33, 165-176; d) J. C. Tebby, in *Comprehensive Heterocyclic*

- Chemistry II* (Eds.: A. R. Katritzky, C. W. Rees, E. F. V. Scriven), Pergamon, Oxford, **1996**, pp. 863–888.
- [2] For recent reviews on the chemistry of PCO<sup>−</sup> see: (a) J. M. Goicoechea, H. Grützmacher, *Angew. Chem. Int. Ed.* DOI: 10.1002/anie.201803888; (b) L. Weber, *Eur. J. Inorg. Chem.* **2018**, 2175–2227.
- [3] a) G. Becker, W. Schwarz, N. Seidler, M. Westerhausen, Z. *Anorg. Allg. Chem.* **1992**, 612, 72–82; b) G. Becker, G. Heckmann, K. Hubler, W. Schwarz, Z. *Anorg. Allg. Chem.* **1994**, 621, 34–46; c) S. Alidori, D. Heift, G. Santiso-Quinones, Z. Benkő, H. Grützmacher, M. Caporali, L. Gonsalvi, A. Rossin, M. Peruzzini, *Chem. Eur. J.* **2012**, 18, 14805–14811; d) F. F. Puschmann, D. Stein, D. Heift, C. Hendriksen, Z. A. Gal, H.-F. Grützmacher, H. Grützmacher, *Angew. Chem. Int. Ed.* **2011**, 50, 8420–8423; e) Y. Lu, H. Wang, Y. Xie, H. Liu, H. F. Schaefer, *Inorg. Chem.* **2014**, 53, 6252–6256; f) F. Tambornino, A. Hinz, R. Köppe, J. M. Goicoechea, *Angew. Chem. Int. Ed.* **2018**, 57, 8230–8234.
- [4] D. Heift, Z. Benkő, H. Grützmacher, *Dalton Trans.* **2014**, 43, 831–840.
- [5] a) A. Hinz, J. M. Goicoechea, *Angew. Chem. Int. Ed.* **2016**, 55, 8536–8541; b) A. Hinz, J. M. Goicoechea, *Angew. Chem. Int. Ed.* **2016**, 55, 15515–15519; c) S. Yao, Y. Grossheim, A. Kostenko, E. Ballester-Martínez, S. Schutte, M. Bispinghoff, H. Grützmacher, M. Driess, *Angew. Chem. Int. Ed.* **2017**, 56, 7465–7469; d) A. Doddi, M. Weinhardt, A. Hinz, D. Bockfeld, J. M. Goicoechea, M. Tamm, *Chem. Commun.* **2017**, 7, 6069–6072; e) M. Joost, W. J. Transue, C. C. Cummins, *Chem. Commun.* **2017**, 53, 10731–10733; f) E. Ballester-Martínez, T. J. Hadlington, T. Szilvási, S. Yao, M. Driess, *Chem. Commun.* **2018**, 54, 6124–6127.
- [6] For representative examples of the chemistry of PCO<sup>−</sup> see: a) A. R. Jupp, J. M. Goicoechea, *J. Am. Chem. Soc.* **2013**, 135, 19131–19134; b) C. Camp, N. Settineri, J. Lefèvre, A. R. Jupp, J. M. Goicoechea, L. Maron, J. Arnold, *Chem. Sci.* **2015**, 6, 6379–6384; c) L. Liu, D. A. Ruiz, D. Munz, G. Bertrand, *Chem. Commun.* **2016**, 1, 147–153; d) L. Liu, D. A. Ruiz, G. Dahcheh, G. Bertrand, R. Suter, A. M. Tondreau, H. Grützmacher, *Chem. Sci.* **2016**, 7, 2335–2341; e) R. Suter, Z. Benkő, H. Grützmacher, *Chem. Eur. J.* **2016**, 22, 14979–14987; f) Z. Li, X. Chen, Z. Benkő, L. Liu, D. A. Ruiz, J. L. Peltier, G. Bertrand, C.-Y. Su, H. Grützmacher, *Angew. Chem. Int. Ed.* **2016**, 55, 6018–6022; g) R. Suter, Y. Mei, M. Baker, Z. Benkő, Z. Li, H. Grützmacher, *Angew. Chem. Int. Ed.* **2017**, 56, 1356–1360; h) L. N. Grant, B. Pinter, B. C. Manor, R. Suter, H. Grützmacher, D. J. Mindiola, *Chem. Eur. J.* **2017**, 23, 6272–6276; i) M. M. Hansmann, D. A. Ruiz, L. Liu, R. Jassar, G. Bertrand, *Chem. Sci.* **2017**, 8, 3720–3725; j) D. W. N. Wilson, A. Hinz, J. M. Goicoechea, *Angew. Chem. Int. Ed.* **2018**, 57, 2188–2193.
- [7] a) A. M. Tondreau, Z. Benkő, J. R. Harmer, H. Grützmacher, *Chem. Sci.* **2014**, 5, 1545–1554; b) T. P. Robinson, M. J. Cowley, D. Scheschkewitz, J. M. Goicoechea, *Angew. Chem. Int. Ed.* **2014**, 54, 683–686.
- [8] a) Z. Mielke, L. Andrews, *Chem. Phys. Lett.* **1991**, 181, 355–360; b) G.-L. Hou, B. Chen, W. J. Transue, Z. Yang, H. Grützmacher, M. Driess, C. C. Cummins, W. T. Borden, X.-B. Wang, *J. Am. Chem. Soc.* **2017**, 139, 8922–8930.
- [9] L. N. Grant, B. Pinter, B. C. Manor, H. Grützmacher, D. J. Mindiola, *Angew. Chem. Int. Ed.* **2018**, 57, 1049–1052.
- [10] C. J. Hoerger, F. W. Heinemann, E. Louyriac, L. Maron, H. Grützmacher, K. Meyer, *Organometallics* **2017**, 36, 4351–4354.
- [11] a) S. R. Waldvogel, M. Selt, *Angew. Chem. Int. Ed.* **2016**, 55, 12578–12580; b) J. D. Wadhwani, F. Marken, R. G. Compton, in *Pure Appl. Chem.*, Vol. 73, **2001**, p. 1947; c) I. Colomer, C. Batchelor-McAuley, B. Odell, T. J. Donohoe, R. G. Compton, *J. Am. Chem. Soc.* **2016**, 138, 8855–8861; d) N. V. Rees, R. Baron, N. M. Kershaw, T. J. Donohoe, R. G. Compton, *J. Am. Chem. Soc.* **2008**, 130, 12256–12257.

- 
- [12] a) R. Guidelli, R. G. Compton, J. M. Feliu, E. Gileadi, J. Lipkowski, W. Schmickler, S. Trasatti, *Pure Appl. Chem.* **2014**, *86*, 245–258; b) R. Guidelli, R. G. Compton, J. M. Feliu, E. Gileadi, J. Lipkowski, W. Schmickler, S. Trasatti, *Pure Appl. Chem.* **2014**, *86*, 259–262; c) D. Li, C. Lin, C. Batchelor-McAuley, L. Chen, R. G. Compton, *J. Electroanal. Chem.* **2018**.
- [13] a) B. A. Brookes, T. J. Davies, A. C. Fisher, R. G. Evans, S. J. Wilkins, K. Yunus, J. D. Wadhawan, R. G. Compton, *J. Phys. Chem. B* **2003**, *107*, 1616–1627; b) T. J. Davies, R. G. Compton, *J. Electroanal. Chem.* **2005**, *585*, 63–82.
- [14] R. G. Compton, C. E. Banks, *Understanding Voltammetry*, 2<sup>nd</sup> ed., Imperial College Press, **2011**.
- [15] R. G. Evans, O. V. Klymenko, S. A. Saddoughi, C. Hardacre, R. G. Compton, *J. Phys. Chem. B* **2004**, *108*, 7878–7886.
- [16] Bruker, TOPSPIN 4.0, <https://www.bruker.com/products/mr/nmr/nmr-software/software/topspin/overview.html>.
-

---

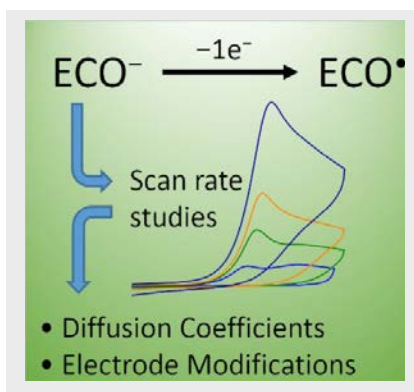
## Entry for the Table of Contents

Layout 1:

## COMMUNICATION

---

The electrochemical behaviour of the heavier cyanate analogues,  $\text{PCO}^-$  and  $\text{AsCO}^-$  is reported in both aqueous and non-aqueous electrolytes.



*Frank Tambornino, Eden E. L. Tanner, Hatem M. A. Amin, Jennifer Holter, Tim Claridge, Richard G. Compton\*, Jose M. Goicoechea\**

**Page No. – Page No.**

**Electrochemical Oxidation of the Phospha- and Arsa-ethynolate Anions,  $\text{PCO}^-$  and  $\text{AsCO}^-$**